JOURNAL OF SOLID STATE CHEMISTRY 99, 166–172 (1992)

# Nonstoichiometry and Phase Relationship of the $SrFeO_{2.5}$–$SrFeO_3$ System at High Temperature

JUNICHIRO MIZUSAKI,* MASANOBU OKAYASU,†
SHIGERU YAMAUCHI,‡ AND KAZUO FUEKI§

*Department of Industrial Chemistry, Faculty of Engineering, University of Tokyo, Hongo, Bunkyo-ku, Tokyo 113, Japan*

Received March 18, 1991; in revised form January 13, 1992; accepted January 17, 1992

In order to make clear the phase relationships and nonstoichiometry of the $SrFeO_{2.5}$–$SrFeO_3$ system at elevated temperatures, measurements were made using high-temperature gravimetry and high-temperature powder X-ray diffraction (XRD) analysis under the controlled oxygen partial pressure of $1–10^{-5}$ atm at temperatures above 400°C. At 400–900°C, the system was found to consist of the $SrFeO_{2.5+\delta}$ phase of the brownmillerite-type structure with small oxygen excess-type nonstoichiometry and the $SrFeO_{3-\delta}$ phase of the cubic perovskite-type structure with large oxygen deficient-type nonstoichiometry. At temperatures above 900°C, the brownmillerite phase transformed to the perovskite-type and the system was composed of only the cubic perovskite-type phase. 

## 1. Introduction

So far, many studies have been made on the $SrFeO_{2.5}$–$SrFeO_3$ system. The system was considered to be composed of largely two types of oxides, nonstoichiometric perovskite-type $SrFeO_{3-\delta}$ and a modified perovskite-type $SrFeO_{2.5}$ (*1–3*).

* To whom correspondence should be addressed. Present address: Institute of Environmental Science and Technology, Yokohama National University, 156 Tokiwadai, Hodogaya-ku, Yokohama 240, Japan.

† Present address: NTT Opto-electronics Laboratories, Nippon Telegraph and Telephone Co., 3-1 Morinosato Wakamiya, Atsugi-shi, Kanagawa 243-01, Japan.

‡ Present address: Research Institute, National Rehabilitation Center for the Disabled, Namiki, Tokorozawa, Saitama 359, Japan.

§ Present address: Department of Industrial Chemistry, Faculty of Science and Technology, Science University of Tokyo, Noda-shi, Chiba 278, Japan.

0022-4596/92 $5.00



$SrFeO_{2.5}$ has been of interest because of its structural features. It shows the orthorhombic brownmillerite structure (*1*). The structure is basically perovskite-type which is composed of the stacks of corner-shared $FeO_6$-octahedra. In the brownmillerite structure, alternate corner-sharing oxygen of $FeO_6$-octahedra in alternate *a–c* planes are missing. Consequently, the structure along the *b*-axis is alternate stacks of the planes composed of $FeO_6$-octahedra and the planes composed of the distorted $FeO_4$-tetrahedra (*4, 5*).

It was shown that the stoichiometric $SrFeO_3$ is a metallic conductor (*1*) in which the valence state of iron ions is 4+, an anomalous state which does not appear in the simple Fe–O system. Electric and magnetic properties change remarkably with the change in oxygen content in $SrFeO_{3-\delta}$ (*2, 3*). Many works have been made using

Mössbauer spectroscopy (*1, 6–9*) and magnetic susceptibility measurement (*2, 3, 7, 8, 10*). $SrFeO_{3-\delta}$ shows large oxygen-deficient-type nonstoichiometry (*2, 3*) and the stoichiometric composition ($\delta = 0$) can be obtained only under high $O_2$ pressure (*2, 9*). Under ordinary pressure, the composition is always oxygen-deficient and the composition of the sample slowly cooled in air to room temperature was reported to be $SrFeO_{2.80}$–$SrFeO_{2.85}$ (*2, 8, 9*).

The reported structure of the $SrFeO_{3-\delta}$-phase at room temperature is rather complicated (*1, 2, 8, 9, 11*). According to the recent report by Takeda *et al.* (*9*), at room temperature, nonstoichiometric perovskite-type $SrFeO_{3-\delta}$ has three modifications with different amounts of oxygen deficiency: cubic perovskite for $0 < \delta < 0.03$, a tetragonal phase for $\delta = 0.125$, and an orthorhombic phase for $\delta = 0.25$. Tofield *et al.* (*11*) showed by the electron diffraction study that the oxygen defect in the orthorhombic $SrFeO_{2.75}$ ($\delta = 0.25$) is ordered.

Takeda *et al.* (*9*) reported the phase relationship at temperatures below 400°C. Also, they showed that the brownmillerite phase changes to the perovskite phase at temperatures around 850–900°C (*9*). However, the relationships between oxygen nonstoichiometry and high-temperature phase relationships between the perovskite-type phases and brownmillerite phase have not been shown yet.

In this paper, we report the phase relationships of the $SrFeO_{2.5}$–$SrFeO_3$ system at temperatures above 400°C determined by high-temperature gravimetric and high-temperature XRD measurements, both under controlled oxygen partial pressure, $P(O_2)$ (*12*).

So far as the authors have searched in literature, it seems there have been few works in which the high-temperature XRD studies were made on oxides as a function of $P(O_2)$ by *in situ* measurement under the precisely controlled low $P(O_2)$ atmospheres.

## 2. Experimental

### *2.1. Samples*

Samples were prepared by a coprecipitation method: Aqueous strontium and iron nitrates were mixed together in 1/1 metallic ratio and poured into $NH_4OH$–$(NH_4)_2C_2O_4$ solution to form the coprecipitate of hydroxides and oxalates. The coprecipitate was kept at 30–45°C for 3–5 days in the $NH_4OH$–$(NH_4)_2C_2O_4$ solution for the fine particles to coagulate, then filtrated and dried. The coprecipitate was heated at temperatures from 300 to 700°C stepwise, holding for 1 hr at every 100°C, at 800°C for 3 hr, and finally at 1200°C for 48 hr.

The calcined oxides were pressed and slightly sintered at 900°C for 7 hr in air and cooled in the furnace at a rate of 30–40 K/hr to room temperature. By the room-temperature powder X-ray analysis, the structure of the formed oxide was perovskite-type.

Other details of the preparation procedures are essentially the same as those reported in the preceding works (*13, 14*).

### *2.2. High-Temperature Gravimetry*

For the determination of equilibrium weight by high-temperature gravimetric measurements, two systems were employed, both with electric microbalance (Shimazu TG 31H). One was equipped with a low-pressure gas-circulation system (*14*). The other was equipped with a flow system of the gas mixtures under ordinary pressure and a zirconia sensor to monitor the oxygen partial pressure of the gas mixtures (*15*).

Oxygen partial pressure was controlled by the use of $Ar$–$O_2$ and $CO$–$CO_2$ gas mixtures of desired ratios. The measurements were made at temperatures of 400–1100°C

using samples of 0.5–1 g. Details of the apparatus and the measuring procedures were essentially the same as those described in the previous papers (*14, 15*).

### *2.3. High-Temperature X-ray Analysis*

High-temperature powder X-ray diffraction (XRD) analysis was made using a Geigerflex-type apparatus (RIGAKUDENKI Co.) equipped with the attachment of a sample heating element (RIGAKUDENKI Co.). The attachment was constructed so that the samples are completely sealed from the outside and the gas mixtures of arbitrary concentrations are allowed to flow inside the sample chamber.

In this work, $N_2$–$O_2$ gas mixtures of desired ratios were let flow to control the atmosphere of the sample. The $P(O_2)$ of outlet gas was monitored by a zirconia sensor to confirm that the atmosphere in the chamber was controlled at the desired $P(O_2)$. The temperature of the sample was controlled using a Pt–PtRh thermocouple attached to the platinum sample holder.

Measurements were made using Cu$K\alpha$ radiation(35kV 15mA) at temperatures up to 950°C in the $P(O_2)$ of $1–10^{-4}$ atm. In order to confirm the equilibrium, the sample was kept at constant $P(O_2)$ and temperature for a long time to make sure that the XRD peaks did not change over several hours. When the composition of the sample changed remarkably, it took more than 1 day to attain equilibrium.

## 3. Results and Discussion

### *3.1. Nonstoichiometry*

*3.1.1. Determination of absolute oxygen content.* Figure 1 shows the oxygen content of the $SrFeO_{2.5}$–$SrFeO_3$ system as a function of log $P(O_2)$ at different temperatures determined by high-temperature gravimetry. The absolute oxygen content in the figure was determined based on the following considerations.

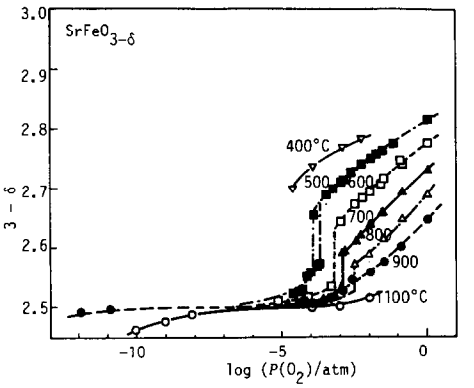


FIG. 1. Oxygen nonstoichiometry of $SrFeO_{2.5}$–$SrFeO_3$ system.

It is known that the plot of oxygen content against log $P(O_2)$ of $La_{1-x}Sr_xFeO_{3-\delta}$ ($0.1 < x < 0.6$) shows two plateaus, at $\delta = 0$, which appears at the $P(O_2)$ region a little higher than 1 atm, and $\delta = x/2$ in the reduced atmospheres (*14, 16*). With increase in $x$ and $T$, the $P(O_2)$ corresponding to the plateaus increases and the plateau at $\delta = 0$ becomes difficult to be observed at high temperatures. When the $La_{1-x}Sr_xFeO_{3-\delta}$ samples ($0.1 < x < 0.6$) were cooled gradually in 1-atm $O_2$ gas in the gravimetry apparatus, the weight saturated at about 200°C and the saturation was attributed to the stoichiometry of $\delta = 0$ (*14, 15*).

As shown in Fig. 2, the tendency of the weight change of $SrFeO_{3-\delta}$ with log $P(O_2)$ at temperatures above 900°C is similar to that of $La_{1-x}Sr_xFeO_{3-\delta}$ (*14, 17*). However, only one plateau is clearly observed which corresponds to $\delta = x/2$ of $La_{1-x}Sr_xFeO_{3-\delta}$. When the sample was cooled down to room temperature in the gravimetry apparatus, the weight gradually increased, and due to the slow reaction rate of oxidation, the accurate equilibrium could not be confirmed below 200°C. Thus, we could not

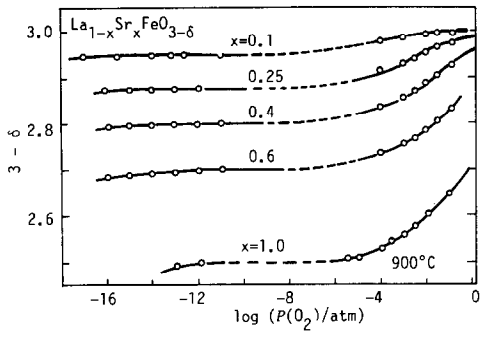


FIG. 2. Oxygen nonstoichiometry of $La_{1-x}Sr_xFeO_{3-\delta}$ at 900°C as a function of log $P(O_2)$. The data points are cited from the original data of Refs. (*14*) and (*17*).

find the saturation of weight corresponding to $\delta = 0$.

For $SrFeO_{3-\delta}$, $x$ in $La_{1-x}Sr_xFeO_{3-\delta}$ is 1. Then, in this work, we consider the plateau observed at 900 and 1100°C as the one corresponding to $\delta = x/2 = 1/2$, and assigned the point of minimum $\partial\,\delta/\partial \ln P(O_2)$ (*14, 15, 18*) as exactly the point of $\delta = 0.500$ or the point corresponding to the composition of $SrFeO_{2.500}$.

The oxygen content in Fig. 1 was calculated from the weight change and the above assignment. By this assignment, the composition of the sample slowly cooled in air to room temperature was $SrFeO_{2.83-2.87}$, which is essentially the same as those reported by the preceding investigators (*2, 8, 9*).

*3.1.2. Nonstoichiometry and phase relationships determined by gravimetry.* As shown in Fig. 1, at temperatures between 400 and 900°C, the $SrFeO_{2.5}$–$SrFeO_3$ system is composed of two different phases, the oxide with the higher oxygen content and with large nonstoichiometry range and the oxide with the composition close to $SrFeO_{2.5}$ and with narrow nonstoichiometry range. The data in Fig. 1 is replotted in the styles of phase diagrams in Figs. 3 and 4: Fig. 3 shows the temperature, $T$, vs composition diagram in which equi-$P(O_2)$ curves are shown, and Fig. 4 shows the log $P(O_2)$ vs $T^{-1}$ plot where equi-$\delta$ lines are indicated.

### *3.2. High-Temperature X-ray Analysis under Controlled Atmosphere*

As to the phase relationships for $T >$ 800°C, the results of high-temperature gravimetry revealed only a vague outline. In order to make clearer the phase relationship, we used the high-temperature XRD data.

Figure 5a shows the temperature change of the XRD peaks between $2\theta = 30$–$33°$ at log $P(O_2)$/atm = −4.7. With an increase in temperature, the cubic perovskite phase changes to the brownmillerite phase between 400 and 500°C and the brownmillerite phase is transformed to the perovskite-type between 850 and 900°C. Figures 5b and 5c show the change in XRD peaks with temperature at log $P(O_2)$/atm = −3.8 and −2.7, respectively. We see that the transition tem-

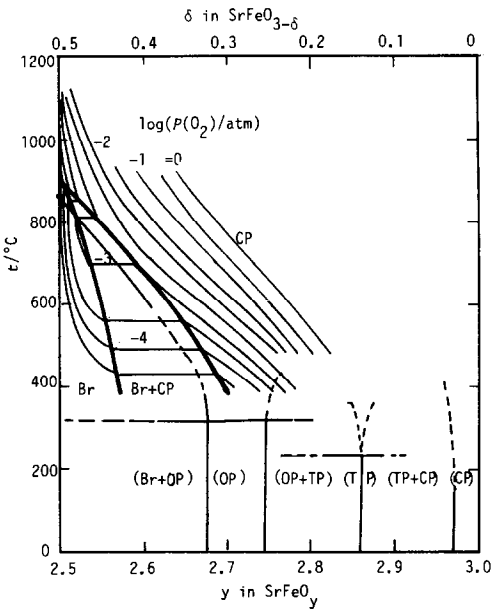


FIG. 3. Phase diagram of the $SrFeO_{2.5}$–$SrFeO_3$ system. Equi-$P(O_2)$ lines are indicated. The phase boundaries proposed by Takeda *et al.* (*9*) are shown by thin lines. Br, brownmillerite phase; CP, cubic perovskite phase; OP, orthorhombic perovskite phase; TP, tetragonal perovskite phase. The phases in parenthesis were proposed by Takeda *et al.* (*9*).

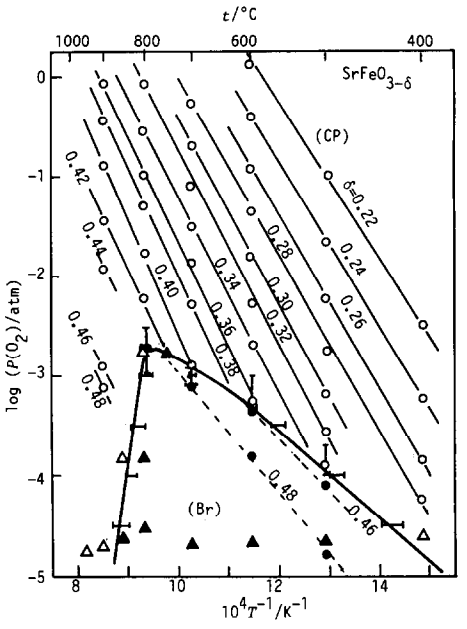


FIG. 4. Equilibrium diagram of the $SrFeO_{2.5}$–$SrFeO_3$ system. The equi-δ lines in $SrFeO_{3-\delta}$ are shown. Symbols of △ and ▲ indicate the results of the high-temperature XRD analysis. Open and closed symbols, respectively, indicate the perovskite-type and the brownmillerite phase, respectively.

perature above 800°C of the brownmillerite phase to cubic perovskite phase decreases with increasing $P(O_2)$.

The data points expressed by △ and ▲ in Fig. 4 show the $P(O_2)$ and temperature determined by the XRD study at which the transition takes place between the brownmillerite phase and perovskite phases. The phase boundary curves indicated in Figs. 3 and 4 are determined so as to be consistent with both thermogravimetry data and the high-temperature XRD data.

The calculated lattice parameters are shown by the data points in Fig. 6 as a function of temperature. The orthorhombic parameters of the brownmillerite phase, *a*, *b*, and *c*, are divided by $2^{1/2}$, 4, and $2^{1/2}$, respectively, to compare them with cubic perovskite-type lattice parameter.

In Fig. 6, the symbols ● indicate the lattice parameter and unit-cell volume of the cubic perovskite phase: Room temperature data are cited from Ref. (*9*) for $SrFeO_{2.97}$ and other data points are determined for the samples under the conditions indicated by △ in Fig. 4. Since the oxygen content of cubic $SrFeO_{3-\delta}$ corresponding to each data point increases with a decrease in temperature, the change in the cubic lattice parameter may be affected not only by the temperature change but also by the nonstoichiometry change. Although the data includes two effects, we find that the lattice parameter of the cubic perovskite-type phase at high temperatures and low temperatures are essentially continuous, irrespective of the formation of the brownmillerite phase at the intermediate temperatures.

As to the data points for the brownmillerite phase, ○, △, and □, those in the parentheses are obtained at $\log [P(O_2)/\text{atm}] = -2.8$ (750°C) and $-3.8$ (800°C), and other points were determined at $\log [P(O_2)/\text{atm}] = -4.7$. The lattice parameters in the higher $\log P(O_2)$ tend to show larger values. However, in the present work, we could not determine the change in the lattice parameters of the brownmillerite phase with the change in δ, or in equilibrium $P(O_2)$.

### *3.3. Comparison with the Literature Data*

In Fig. 3, the phase diagram determined by Takeda *et al.*by DTA (*9*) is also shown. Both results are largely consistent with each other. Although there are three modifications reported in the perovskite-type phase at temperatures below ca. 350°C, these phases transform to the single phase of the cubic perovskite-type with large oxygen nonstoichiometry above 400°C. The brownmillerite phase shows some extent of oxygen excess-type nonstoichiometry which becomes larger with decreasing in temperature. However, the brownmillerite phase disappears and only the cubic perovskite-

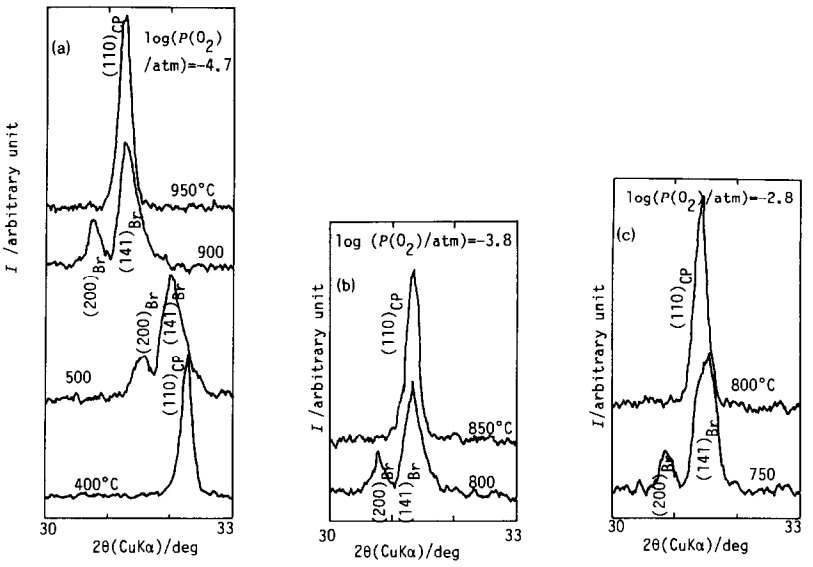


FIG. 5. Phase transition observed by the high-temperature XRD analysis. The suffixes Br and CP indicate the brownmillerite phase and cubic perovskite phase, respectively. (a) log [$P(O_2)$/atm] = −4.7; (b) log [$P(O_2)$/atm] = −3.8; (c) log [$P(O_2)$/atm] = −2.8.

phase of large nonstoichiometry remains above 900°C.

There is a small difference between the results by the present work and those by Takeda *et al.*(9) as to the boundary between the perovskite-type phase and brownmillerite phase. It may be attributed to the difference in the experimental method. Takeda *et al.*(9) prepared the samples by quenching from appropriate temperatures and in certain oxygen pressures. Then, they analyzed the oxygen content by iodometry. It is clear from Fig. 3 that their samples were mostly two-phase mixtures of brownmillerite and perovskite-type phases at room temperature. The samples were then submitted for DTA measurements which were made in 99.99%$N_2$ atmosphere under heating rate of 10°C/min. Therefore, their DTA data were for the nonequilibrium oxide mixtures. On the other hand, the present work was made exactly on the equilibrium state, which may give a more accurate phase boundary.

In Fig. 6, the results of high-temperature XRD results by Takeda *et al.* (9) are shown by the broken lines. The data by the present work are on the equilibrium state with the controlled $P(O_2)$ atmosphere. On the other hand, Takeda *et al.*(9) used brownmillerite $SrFeO_{2.5}$ as a starting sample and made the high-temperature XRD measurement in 99.99%$N_2$ atmosphere, assuming that the oxygen content was kept constant during the measurement. Therefore, their data did not show the perovskite-type phase at the lower temperature region.

Taking into account the difference of the experimental conditions, both sets of results are essentially consistent with each other: The phase-transition temperature is strongly affected by the equilibrium $P(O_2)$. The lattice parameters of the brownmillerite phase tend to increase with the equilibrium $P(O_2)$.

## 4. Conclusion

(1) The phase relationships of the $SrFeO_{2.5}$–$SrFeO_3$ system above 400°C were

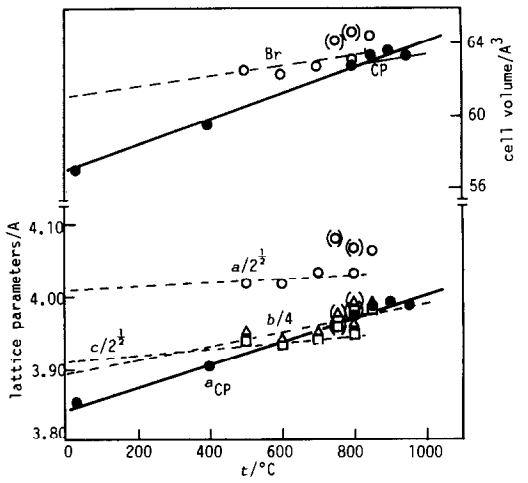


FIG. 6. Lattice parameters (lower part) and unit-cell volume (upper part) as a function of temperature.

Closed symbols: cubic perovskite-type phase. Room-temperature data are for $SrFeO_{2.97}$ cited from Ref. (*9*). Other data are for the conditions indicated in Fig. 4 by △.

Open symbols: brownmillerite phase. In the lower part: ○, $a/2^{1/2}$; △, $b/4$; □, $c/2^{1/2}$. Symbols without ( ) is at log $[P(O_2)/\text{atm}] = -4.7$. Symbols in ( ) at 750 and 800°C, respectively, are at log $[P(O_2)/\text{atm}] = -3.8$ and $-2.8$, respectively. The unit-cell volume for the brownmillerite phase was divided by 8 to compare the value with that of the cubic perovskite phase. Broken lines are cited from the results by Takeda *et al.*(*9*).

determined as a function of temperature and oxygen partial pressure.

(2) At temperatures of 400–900°C, the $SrFeO_{2.5}$–$SrFeO_3$ system consists of two phases, the brownmillerite-type $SrFeO_{2.5}$ phase with small oxygen excess-type nonstoichiometry and the cubic perovskite-type $SrFeO_{3-\delta}$ phase with large oxygen-deficient-type nonstoichiometry. At temperatures above 900°C, the brownmillerite phase decomposes to the perovskite-phase and only the $SrFeO_{3-\delta}$ remains.

(3) The high-temperature *in situ* XRD measurement was made on the sample in equilibrium with the controlled $P(O_2)$ atmosphere. By this measurement, the transformation temperature above 800°C of the brownmillerite phase to the perovskite-type phase was found to increase up to 900°C with decreasing equilibrium $P(O_2)$.

## References


1. P. K. GALLAGHER, J. B. MACCHESNEY, AND D. N. E. BUCHAMAN, *J. Chem. Phys.* **41,** 2429 (1964).
2. J. B. MACCHESNEY, R. C. SHERWOOD, AND J. F. POTTER, *J. Chem. Phys.* **43,** 1907 (1965).
3. H. WATANABE, *J. Phys. Soc. Jpn.***12,** 515 (1957).
4. C. GREAVES, A. J. JACOBSON, B. C. TOFIELD, AND B. E. F. FENDER, *Acta Crystallogr. Sect. B* **31,** 641 (1975).
5. J.-C. GRENIER, J. DARRIET, M. POUCHARD, AND P. HAGENMULLER, *Mater. Res. Bull.* **11,** 1219 (1976).
6. U. SHIMONY AND J. M. KNUDSEN, *Phys. Rev.* **144,** 361 (1966).
7. M. TAKANO, J. KAWACHI, N. NAKANISHI, AND Y. TAKEDA, *J. Solid State Chem.* **39,** 75 (1981).
8. T. C. GIBB, *J. Chem. Soc. Dalton Trans.*, 1455 (1985).
9. Y. TAKEDA, K. KANNO, T. TAKADA, O. YAMAMOTO, M. TAKANO, N. NAKAYAMA, AND Y. BANDO, *J. Solid State Chem.* **63,** 237 (1986).
10. T. TAKEDA, Y. YAMAGUCHI, AND H. WATANABE, *J. Phys. Soc. Jpn.* **33,** 967 (1972).
11. B. C. TOFIELD, C. GREAVES, AND B. E. F. FENDER, *Mater. Res. Bull.* **10,** 737 (1975).
12. The experimental part of this work was already finished in 1985, and the results were referenced by Takeda *et al.* in (*9*) as Ref. (*10*): a private communication by J. Mizusaki.
13. T. SASAMOTO, J. MIZUSAKI, M. YOSHIMURA, W. R. CANNON, AND H. K. BOWEN, *Yogyo Kyokaishi* **90,** 32 (1982).
14. J. MIZUSAKI, M. YOSHIHIRO, S. YAMAUCHI AND K. FUEKI, *J. Solid State Chem.* **58,** 257 (1985).
15. J. MIZUSAKI, Y. MIMA, S. YAMAUCHI, AND K. FUEKI, *J. Solid State Chem.* **80,** 102 (1989).
16. In the caption of Fig. 3 of Ref. (*14*), the composition was wrongly indicated by the present author. $La_{0.75}Sr_{0.25}FeO_{3-\delta}$ in the caption should be read as $La_{0.4}Sr_{0.6}FeO_{3-\delta}$.
17. J. MIZUSAKI, M. YOSHIHIRO, S. YAMAUCHI, AND K. FUEKI, *J. Solid State Chem.* **67,** 1 (1987).
18. C. WAGNER, *Prog. Solid State Chem.* **6,** 1 (1971).